# Structural investigation and improvement of microwave dielectric properties in $Ca_{1-x}Ba_xTiO_3$, low loss ceramics

**Sarir Uddin[a,†], Abid Zaman[b,†,*], Imtiaz Rasool[c], Sadiq Akbar[c], Muhammad Kamran[c], Nasir Mehboob[b], Asad Ali[b], Abid Ahmad[b], Muhammad Farooq Nasir[b] and Zafar Iqbal[b]**

[a]*Department of Physics, Government College Hayatabad, Peshawar 25000, Pakistan*
[b]*Department of Physics, Riphah International University, Islamabad 44000, Pakistan*
[c]*Department of Electronics, University of Peshawar, 25120, Pakistan*

**The effects of Ba substitution on the phase analysis, microstructure and microwave dielectric properties of $Ca_{1-x}Ba_xTiO_3$ ceramics were prepared through conventional solid state reaction route. The X-ray diffraction analysis of the samples showed that the specimens $Ca_{1-x}Ba_xTiO_3$ presented single phase compound with orthorhombic structure in the range of x=0.0 to 0.7 when sintered at 1300°C for 3hrs in air. From the morphological point of view, it consists of round and rod shaped grains with porous microstructure. The substitution of $Ba^{2+}$ ions over $Ca^{2+}$, the microwave dielectric constant ($\varepsilon_r$) diminishes from 145 to 52 whereas the quality factor (Qxf) will increases from 8105 to 24305 GHz and temperature coefficient of resonant frequency decreases from 705 to 80 ppm/°C (at 3 GHz).**

**Keywords: $CaTiO_3$, Solid State Reaction Route, Crystal structure, Microstructure, Dielectric Properties.**

## Introduction

The last couple of decades, the rapid developments of microwave communication technology such as several different wireless communication, rapid production of low-cost, lightweight, television receiver only (TVRO, 2-5 GHz), direct broadcasting (DBS, 11 GHz to 13 GHz) and high reliable devices [1, 2]. The necessity for miniature low loss microwave devices has led to the dielectric material loading of cavity resonator, using dielectric resonators [3, 4]. These dielectric resonators should satisfy three foremost criteria; viz a high dielectric constant for size miniaturization, a low dielectric loss for good selectivity and temperature coefficient of resonant frequency is close to zero for stable frequency stability [5].

Calcium titanium oxide $CaTiO_3$ (CT) is an excellent ceramic for microwave (MW) dielectric since it has a large permittivity $\varepsilon_r = 160$ and an allowable quality factor, $Q = 8,000$ at 1.5 GHz. But unfortunately its feature is a high positive temperature co-efficient of the resonant frequency $\tau_f = +850$ ppm K$^{-1}$ [6, 7]. The dielectric properties of $CaTiO_3$ ceramics will be further improved by introducing isovalent substitution like $Sr^{+2}$, $Mg^{+2}$ or $Ba^{+2}$ at A-site of $ABO_3$ perovskite-structured $CaTiO_3$ [8].

An alternative $MgTiO_3$ ceramics material has attracted enormous contemplation because of its good microwave dielectric properties and far low cost. The dielectric constant $\epsilon_r = 17$, quality factor $Q \times f = 160,000$ GHz and temperature coefficient of resonant frequency $\tau_f = -50$ppm/°C are achieve for $MgTiO_3$ ceramics [9]. The doping A-site, with elements like Ni, Co and Zn led to enrichment within the $Q \times f$ value of $MgTiO_3$(180,000 GHz to 364,000 GHz), $\epsilon_r = 17.2$ and $\tau_f \sim -45$ ppm/°C [10, 11].

Another promising example of advanced ceramics $(1-x)CaTiO_3–xLaAlO_3$ ($0 \leq x \leq 1$) solid solution. The dielectric constant "$\epsilon_r$" decrease from 47.83 to 28.25, $Q \times f$ increase from 30,000 to 42,000GHz and the value of temperature co-efficient of the resonant frequency "$\tau_f$" decreases from 17.77 to -20.42 ppm/°C because the $LaAlO_3$ contented within the CTLA ceramics increased and the polarizability alteration decreases from 1.74 to 5.0% by the increase of $LaAlO_3$ [12]. The others compounds with microwave dielectric properties are shown in Table 1.

A few approaches are received for the synthesis of $CaTiO_3$ either by soft chemistry like Sol-gel or by hydrothermal or solvothermal methods, co-precipitation, or organic-inorganic solution [14-17]. High temperature solid state synthesis of $CaTiO_3$ has been conducted utilizing the mixtures of calcium carbonate ($CaCO_3$) and titanium dioxide ($TiO_2$) [18-20].

In the present work, the results on the microstructure improvement and dielectric properties of $CaTiO_3$ ceramics is reported. The results prove that the dielectric

[†]These authors contributed equally to this work.
*Corresponding author:
 Tel : + 0092334825 7783
 E-mail: zaman.abid87@gmail.com

**Table 1.** Dielectric material with compound with its different properties [13].

| Compound | Sintering Temperature ($^\circ$C) | Permittivity ($\varepsilon_r$) | Qxf (GHz) | $\tau_f$ (ppm/$^\circ$C) |
|---|---|---|---|---|
| $CaTiO_3$ | 1400 | 160 | 7,000 | 850 |
| $Ba_2Ti_9O_{20}$ | 1350 | 39 | 32,000 | 2 |
| $BaTi_4O_9$ | 1300 | 37 | 22,700 | 15 |
| $BaTi_5O_{11}$ | 1120 | 42 | 61,110 | 39 |
| $Ca_3ZrSi_2O_9$ | 1400 | 10.6 | 93,300 | -77 |
| $Ca_3SnSi_2O_9$ | 1400 | 8.6 | 54,800 | -65 |

properties especially the temperature coefficient of resonant frequency of the $CaTiO_3$ materials are improved noticeably.

## Experimental Procedure

The samples were arranged through mixed compound solid state technique as a result it's the only, the best and economically route utilized in industries. According to the formula $Ca_{1-x}Ba_xTiO_3$ ($0 \leq x \leq 0.7$) with the highly pure materials of $CaCO_3$ (SIGMA-ALDRICH), $BaCO_3$ (SIGMA-ALDRICH) and $TiO_2$ (SIGMA-ALDRICH) with purity $\geq 99.5\%$. The powders were horizontal ball milled in polymer bottle with distilled water and zirconia balls for 12 h. After the drying method (90 $^\circ$C for 24 h), the powder were grinded and then calcined at 950 $^\circ$C for the composition with x = 0 and 1,000 $^\circ$C for the compositions with ($0 \leq x \leq 0.7$) for 3 h at a heating/ cooling rate of 5 $^\circ$C/min. At that point calcined fine powders (0.5-0.7 g) within the size of 10 mm diameter and in the thickness 3-4 mm pellets, under the pressure of 100 MPa with a stainless steel dye during a Carver Manual Uniaxial press. The pellets were placed on ceramic foil and sintering at 1,300 $^\circ$C for 3 h at heating/ cooling rate of 5 $^\circ$C/min.

The phase analyses of the samples were carried out via X-rays diffractometer (XRD) (JDX-3532, JEOL Japan) with Cu-K$\alpha$ radiations ($\lambda$ = 1.540598 Å), operated at 45 kV and 40 mA was utilize for identification of phases. A step size 0.05$^\circ$, a scan rate of 0.5$^\circ$/min and scan ranges of 10.015-70.015$^\circ$ were embraced. The microstructures of the sample were analyzed by scanning electron microscopy (SEM) (JDX-5910, JEOL Japan). For SEM, samples were polished and thermally etched at temperatures 10% less than their sintering temperatures for 1 h. The apparent bulk densities of sintered samples were measured by Archimedes method using densitometer (MD 300s). The microwave dielectric properties of the fabricated ceramic pellets were measured by Vector Network Analyzer (Agilent-R3767CH).

## Results and Discussion

### Phase formation analysis

Fig. 1 shows the XRD patterns of $Ca_{1-x}Ba_xTiO_3$ ceramics sintered at 1,300 $^\circ$C for 3 h in air where x = 0.0, 0.1, 0.2, 0.3, 0.4, 0.5, 0.6 and 0.7. At this sintering temperature, all the samples well developed orthorhombic phase structures was detected for $Ca_{1-x}Ba_xTiO_3$ ($0 \leq x \leq 0.4$) but in $Ca_{1-x}Ba_xTiO_3$ ($x \geq 0.5$) the orthorhombic phase was found. It was observed that the crystal structure of the synthesized ceramic samples changed from orthorhombic space group (Pbnm) to orthorhombic space group (Pnab) with the variation of barium concentration [21, 22]. Besides, with the increasing of "x" the peaks in XRD spectra slowly shifted to lower angle. It's because of that ionic radii of $Ba^{2+}$ ions (r = 1.61 Å) are larger than that of $Ca^{2+}$ ions (r = 1.34 Å) [23]. The diffraction peaks in the XRD patterns can be indexed that belonged to the space group (Pnma) and (Pbnm) matching with pdf card # (22-153) and (78-1013) respectively. With increasing x from 0 to 0.7, the lattice parameters 'a', 'b' and 'c' changes almost linearly $CaTiO_3$ to $Ca_{1-x}Ba_xTiO_3$. The variation in the
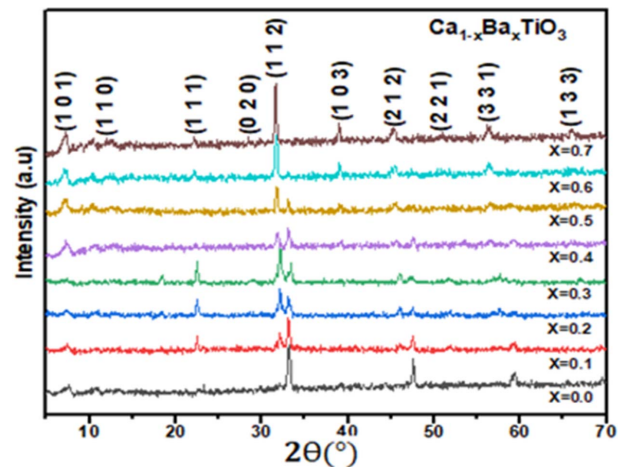


**Fig. 1.** XRD patterns of the $Ca_{1-x}Ba_xTiO_3$ ($0 \leq x \leq 0.7$) ceramics sintered at 1,300 $^\circ$C in air.
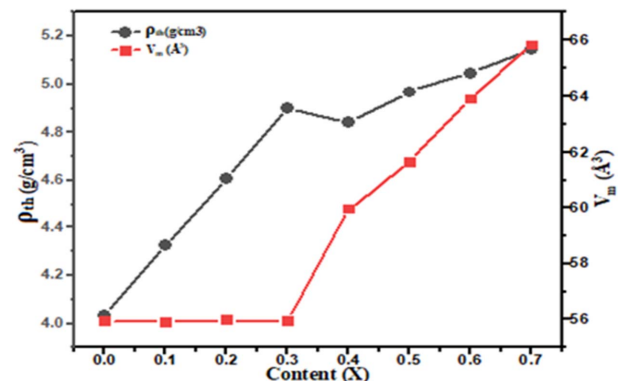


**Fig. 2.** Plot of theoretical density ($\rho_{th}$) and Molar volume ($V_m$) with different concentration $Ba^{2+}$ content "x".

**Table 2.** Structural Data of Ca$_{1-x}$Ba$_x$TiO$_3$ ceramics from XRD Analysis sintered at 1,300 °C.

| X | a(Å) | b(Å) | c(Å) | Z | Structure | S.G | V$_{unit}$ (Å$^3$) | V$_m$ (Å$^3$) |
|---|---|---|---|---|---|---|---|---|
| 0.0 | 5.4405 | 7.6436 | 5.3812 | 4 | Orthorhombic | Pnma | 223.7772 | 55.94431 |
| 0.1 | 5.3796 | 5.4423 | 7.6401 | 4 | Orthorhombic | Pbnm | 223.6822 | 55.92056 |
| 0.2 | 7.9800 | 5.5900 | 5.0200 | 4 | Orthorhombic | Pbnm | 223.9332 | 55.98329 |
| 0.3 | 5.4424 | 7.6417 | 5.3807 | 4 | Orthorhombic | Pbnm | 223.7789 | 55.94474 |
| 0.4 | 5.6138 | 6.6836 | 6.3912 | 4 | Orthorhombic | Pbnm | 239.8003 | 59.95009 |
| 0.5 | 5.0839 | 5.8011 | 7.1068 | 4 | Orthorhombic | Pbnm | 246.7002 | 61.67505 |
| 0.6 | 8.1301 | 5.8436 | 5.3812 | 4 | Orthorhombic | Pnab | 255.6557 | 63.91393 |
| 0.7 | 5.0198 | 6.5381 | 8.0232 | 4 | Orthorhombic | Pnab | 263.3211 | 65.83026 |

X = Ba$^{2+}$ content, Z = No. of atom per unit cell, S.G = Space group, V$_{unit}$ = Volume of unit cell, V$_m$ = Molar volume, a, b & c = Lattice Parameters

**Table 3.** MW dielectric properties of the fabricated Ca$_{1-x}$Ba$_x$TiO$_3$ samples sintered at 1,300 °C.

| X | S.T (°C) | ρ$_{exp}$ (g/cm$^3$) | ρ$_{th}$ (g/cm$^3$) | ρ$_{rel}$ (%) | (ε$_r$) | Qxf (GHz) | Tan δ | τ$_f$ (ppm/°C) |
|---|---|---|---|---|---|---|---|---|
| 0.0 | 1,300 °C | 3.724 | 4.035 | 92.28 | 145 | 8105 | 0.0001234 | 705 |
| 0.1 | 1,300 °C | 4.036 | 4.326 | 93.30 | 138 | 10120 | 0.0000988 | 670 |
| 0.2 | 1,300 °C | 4.125 | 4.609 | 89.49 | 125 | 12500 | 0.0000800 | 625 |
| 0.3 | 1,300 °C | 4.212 | 4.901 | 85.94 | 108 | 14240 | 0.0000702 | 550 |
| 0.4 | 1,300 °C | 4.365 | 4.842 | 90.13 | 95 | 17100 | 0.0000585 | 455 |
| 0.5 | 1,300 °C | 4.602 | 4.969 | 92.61 | 80 | 19400 | 0.0000515 | 340 |
| 0.6 | 1,300 °C | 4.805 | 5.048 | 95.19 | 65 | 21920 | 0.0000456 | 215 |
| 0.7 | 1,300 °C | 5.031 | 5.146 | 97.76 | 52 | 24305 | 0.0000411 | 80 |

X = Ba$^{2+}$ content, S.T = Sintering Temperature, ρ$_{exp}$ = Experimental density, ρ$_{th}$ = Theoretically density, ρ$_{rel}$ = Relative density

lattice parameters 'a', 'b' and 'c' of the Ca$_{1-x}$Ba$_x$TiO$_3$ ceramics with the increase in Ba$^{2+}$ content is shown in Table 2. The variation of theoretical density (ρ$_{th}$) and molar volume (V$_m$) as a function of x is shown in Fig. 2. The theoretical density (ρ$_{th}$) increases due to the replacement of lighter atomic mass Ca$^{+2}$ ions unit cell for the higher atomic mass Ba$^{+2}$ ions.

**Microstructural analysis**

Fig. 3 represents the surface morphology of CBT at different barium content (x) where (x = 0.0, 0.1, 0.2, 0.3, 0.4, 0.5, 0.6, and 0.7) for the prepared samples by mixed oxide solid state reaction route sintered at 1,300 °C for 3 h in air. In Fig. 3 the SEM images have show that microstructure consists of round-like and rod shaped grains with little pores microstructure in the range of 1 × 1 μm$^2$ to 3 × 3 μm$^2$ sizes. The grains are homogeneous and the surface is smooth in the range x = 0.3 and 0.5 as shown in Fig. 3(d, e, f). The presence of some bigger grains are often observed within the Fig. 3(a, b, c) sintered at 1,300 °C which may be due to calcium titanate attempting to diminish the internal energy by reducing the full area of grain boundary, resulting in the subsequent grain growth [24]. This implies that the substitution of Ba$^{2+}$ over Ca$^{2+}$ in perovskite lattice can demote the grain growth as shown in Fig. 3(g, h). This type of morphology has been previously reported for CaTiO$_3$ ceramics [25].

**Microwave dielectric analysis**

The microwave dielectric properties of Ca$_{1-x}$Ba$_x$TiO$_3$ (0 ≤ x ≤ 0.7) ceramics sintered at 1,300 °C for 3 h was measured with an operating frequency of 3 GHz compared with Table 3. The obtained dielectric constant (ε$_r$) for Ca$_{1-x}$Ba$_x$TiO$_3$ where (x= 0.0, 0.1, 0.2, 0.3, 0.4, 0.5, 0.6, and 0.7) decreases from 145 to 52 at 3 GHz frequency are shown in Fig. 4. This indicated that a small amount of barium doping decreased the dielectric constant value of ceramic. In Fig. 5(a) shows the quality factor (Q × f) of Ca$_{1-x}$Ba$_x$TiO$_3$ ceramics with different content x. The quality factor (Qxf) increases from 8105 to 24305 GHz with increase in barium concentration. The maximum value of Qxf as 24,305 GHz was obtained for the Ca$_{0.3}$Ba$_{0.7}$TiO$_3$ ceramics sintered at 1,300 °C for 3hrs. In Fig. 5(b) shown the temperature coefficient of resonant frequency (τ$_f$) decrease from 705 to 80 ppm/°C, with increase in Ba$^{2+}$ concentration, assume that due to the lower ionic polarizability of Ca$^{+2}$ (3.16 Å$^3$) compared with Ba$^{+2}$ (6.40 Å$^3$) [26]. In Fig. 4 the dielectric constant was observed to follow the relative density and (ε$_r$) ~ 52 was obtained for the ~ 97.76% dense ceramics with x = 0.7. In general, Q × f increases when smaller cations are replaced by larger cations because larger cations cause a rise within the movement of A-site cations resulting to an increase in dielectric losses and therefore a decrease in Qxf [27].
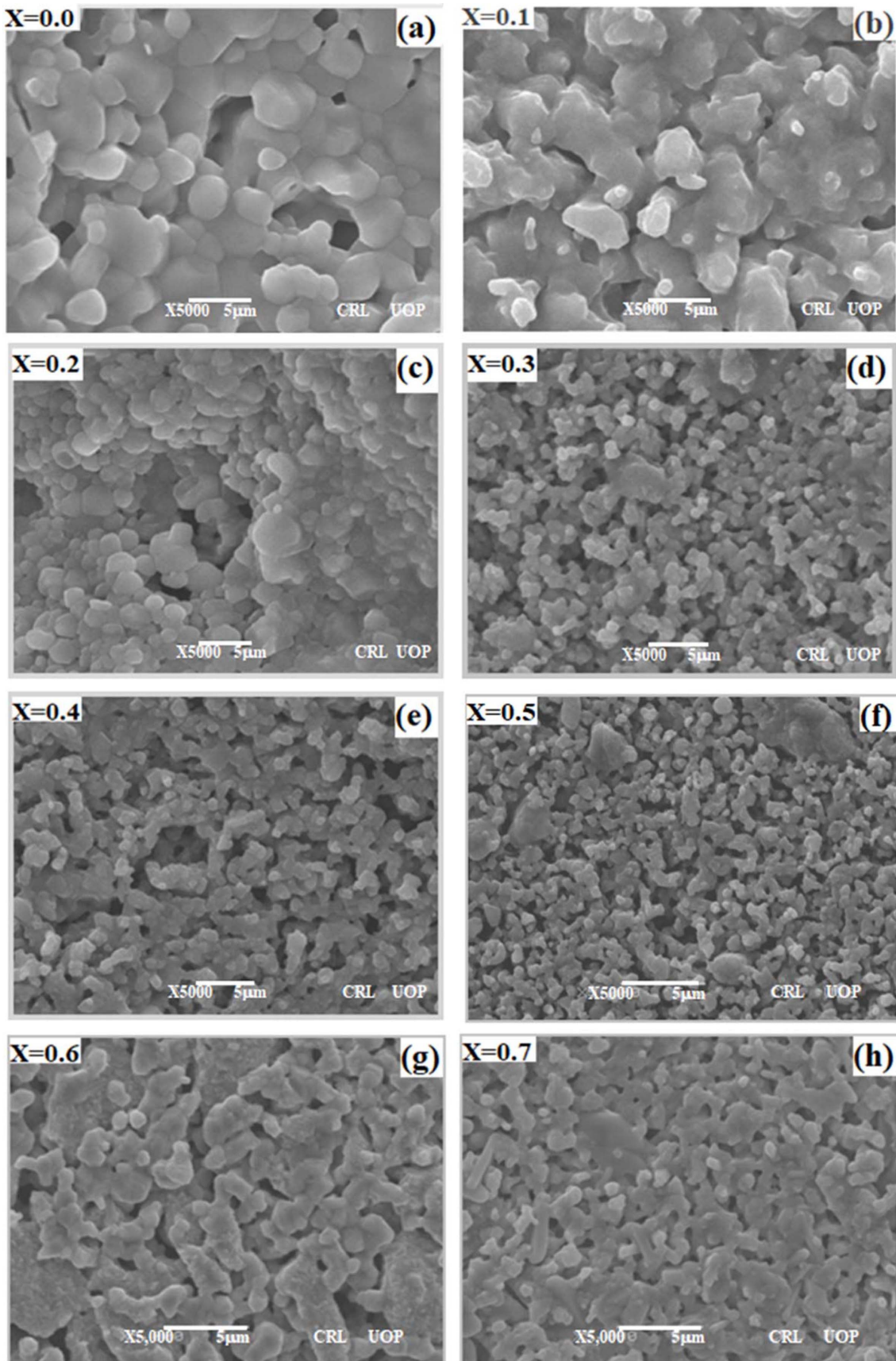
**Fig. 3.** SEM micrograph of the $Ca_{1-x}Ba_xTiO_3$ $0 \leq x \leq 0.7$) ceramics sintered at 1300 °C for 3hrs in air; (a) x = 0.0, (b) x = 0.1, (c) x = 0.2, (d) x = 0.3, (e) x = 0.4, (f) x=0.5, (g) x=0.6, (h) x=0.7; indicating a slight change in grain sizes with increase in x.
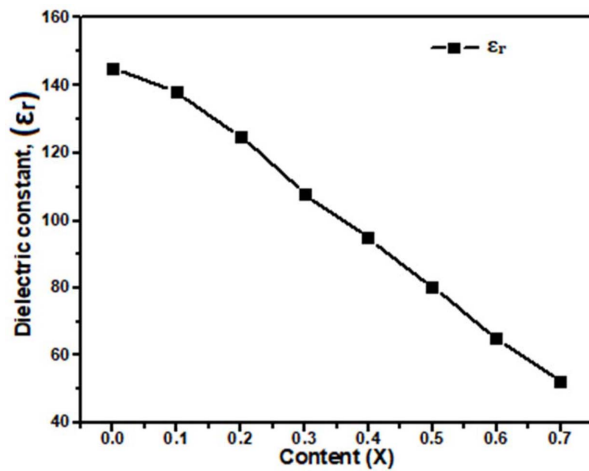
**Fig. 4.** Plot of dielectric constant ($\varepsilon_r$) versus Ba$^{2+}$ content (x) for Ca$_{1-x}$Ba$_x$TiO$_3$ ($0 \leq x \leq 0.7$).
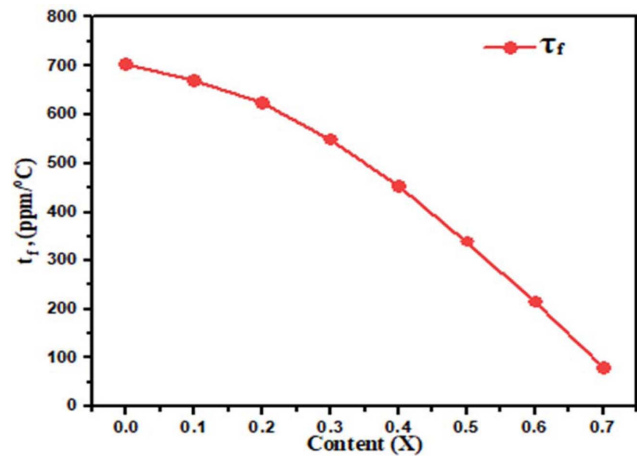


**Fig. 6.** Plot of Temperature coefficient of resonant frequency with different concentration Ba$^{2+}$ content (x).
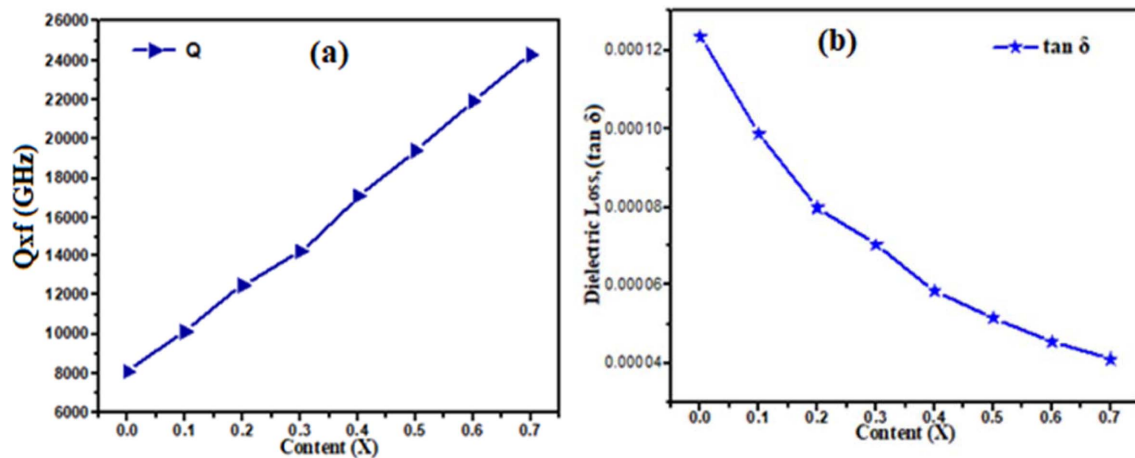


**Fig. 5.** Comparison of (a) Quality factor and (b) Dielectric loss with different concentration Ba$^{2+}$ Content (x)

## Conclusions

Ca$_{1-x}$Ba$_x$TiO$_3$ ($0 \leq x \leq 0.7$) was successfully synthesized by mixed oxide solid state method. Microstructure and microwave dielectric properties of Ca$_{1-x}$Ba$_x$TiO$_3$ system have been studied for the composition variation ($0 \leq x \leq 0.7$). A single phase was obtained of Ca$_{1-x}$Ba$_x$TiO$_3$ ($0 \leq x \leq 0.7$) ceramic sintering at 1,300 ℃ for 3 h in air. The SEM morphology it consists of round and rod shaped grains with porous microstructure. The ceramics samples sintered at 1,300 ℃ for 3 h exhibited a maximum density of 5.146 g/cm$^3$. The dielectric constant ($\varepsilon_r$) decreases from 145 for x = 0.0 to 52 for x = 0.7. The near zero ($\tau_f$) value decreases from 705 to 80 ppm/℃ (at 3 GHz) with an increase in Ba$^{2+}$ concentration from 0.0 to 0.7.

## Acknowledgment

## References

1. R.C Kell, A.C Greenham, and G.C.E Olds, Chem. Inform. 4[38] (1973) 352-354
2. D. Suvorov, M. Valant, B. Jancar, and S.D. Skapin. Acta Chimica Slovenica 48[1] (2001) 87-99.
3. T. Ishizaki, M. Fujita, H. Kagata, T. Uwano and H. Miyake, Microwave theory Tech. 42[11] (1994) 2017-2022.
4. I.M. Reaney and D. Iddles, J. Am. Ceram. Soc. 89[7] (2006) 2063-2072.
5. C.L. Huang, C.F. Tseng, W.R. Yang, and T.J. Yang, J. Am. Ceram. Soc. 91[7] (2008) 2201-2204.
6. C.L Huang, C.L Pan, and S.J Shium, Mater. Chem. Phys. 78[1] (2003) 111-115.
7. R.D. Shennon, Acta crystallographica A. 32[5] (1976) 751-767.
8. A. Zaman, S., Uddin, and N. Mehboob, Iranian J. of Sci. and Tech. Tranc. A: Science (2020) 1-5.
9. K. Wakino, Ferroelectrics 91[1] (1989) 69-86.
10. E.S. Kim and C.J. Jeon. J. of the Eup. Cerm. Soci. 30[2]

(2010) 341-346.

11. C.L. Huang and S.S. Liu. Jap. J. of app. Phy. 46[1] (2007) 283-285.

12. Z. Dou, G. Wang, J. Jiang, F. Zhang, and T. Zhang J. of Adv. Cerm. 6[1] (2017) 20-26.

13. J. Kumar and N. Gupta. Wireless Personal Communi-Cations 75[2] (2014) 1029-1049.

14. P. K. Mallik, G. Biswal, S.C. Patnaik, and S. K. Senapati, IOP Conference Series Materials Science and Engineering 75 (2015) 012005.

15. S. Holliday and A. Stanishevsky, Surf. Coat. Technol. 188-189 (2004) 741-744.

16. D. Wang, Z. Guo, Y. Chen, J. Hao, and W. Liu, Inorganic Chem. 46[19] (2007) 7707-7709.

17. W. Dong, G. Zhao, Q. Bao, and X. Gu, Materials Sci. 21[4] (2015) 583-585.

18. G. Gralik, C. Zanelli, F. Raupp-Pereira, M. Dondi, and D. Hotza, in proceeding of 21 Congresso Brasileiro de Engenharia Materiais, October 2014, p.504-510.

19. M. Sh. Khali and F.F. Hammad, Egypt. J. Solid. 25[2] (2002) 175-183.

20. G. Gralik, A. Thomson, C. Moreas, F. Raupp-Pereira, and D. Hotza, Proc. Appl. Ceram. 8[2] (2014) 53-57.

21. J. Guevarra, A. Schonleber, S.V Smaalen, and F. Lichtenberg, Acta Cryst. B. 63[2] (2007) 183-189.

22. A.R. Drews, W. Wong-Ng, R.S. Roth, and T.A. Vanderah, Mater. Res. Bull. 31[2] (1996) 153-162.

23. P.L. Wise, I.M. Reaney, W.E. Lee, T.J. Price, D.M. Iddles, and D.S. Cannell, Euro. J. Ceram. Soc. 21[10-11] (2001) 1723-1726.

24. J. Varghese, T. Joseph, K. P. Surendran, T. P. D. Rajan, and M. T. Sebastian, D. Trans, Royal Society of Chem. 44[11] (2015) 5146-5152.

25. R.D. Shannon, J. Appl. Phys. 73[1] (1993) 348-366.

26. J. Mitroy, M.S. Safronova, and C. W. Clark, J. of Phys. B Atomic Molecular and Optical Phys. 43[20] (2010) 202001.

27. Y. Tohdo, K. Kakimoto, H. Ohsato, H. Yamada, and T. Okawa, J. Eur. Cerm. Soc. 26[10-11] (2006) 2039-2043.